JACS
JOURNAL OF THE AMERICAN CHEMICAL SOCIETY
Article
pubs.acs.org/JACS

Integrated Approach to Identify Heparan Sulfate Ligand Requirements of Robo1

Chengli Zong,[†,‡] Rongrong Huang,[†,‡] Eduard Condac,[†] Yulun Chiu,[†,§] Wenyuan Xiao,[†,∥] Xiuru Li,[†] Weigang Lu,[†,‡] Mayumi Ishihara,[†] Shuo Wang,[†] Annapoorani Ramiah,[†] Morgan Stickney,[‡] Parastoo Azadi,[†] I. Jonathan Amster,[‡] Kelley W. Moremen,[†,∥] Lianchun Wang,[†,∥] Joshua S. Sharp,[†,⊥] and Geert-Jan Boons*[,†,‡,#]

[†]Complex Carbohydrate Research Center, [‡]Department of Chemistry, [§]Institute of Bioinformatics, [∥]Department of Biochemistry and Molecular Biology, University of Georgia, 315 Riverbend Road, Athens, Georgia 30602, United States

[#]Department of Chemical Biology and Drug Discovery, Utrecht Institute for Pharmaceutical Sciences, and Bijvoet Center for Biomolecular Research, Utrecht University, Universiteitsweg 99, 3584 CG Utrecht, The Netherlands

Supporting Information

ABSTRACT: An integrated methodology is described to establish ligand requirements for heparan sulfate (HS) binding proteins based on a workflow in which HS octasaccharides are produced by partial enzymatic degradation of natural HS followed by size exclusion purification, affinity enrichment using an immobilized HS-binding protein of interest, putative structure determination of isolated compounds by a hydrophilic interaction chromatography−high-resolution mass spectrometry platform, and chemical synthesis of well-defined HS oligosaccharides for structure−activity relationship studies. The methodology was used to establish the ligand requirements of human Roundabout receptor 1 (Robo1), which is involved in a number of developmental processes. Mass spectrometric analysis of the starting octasaccharide mixture and the Robo1-bound fraction indicated that Robo1 has a preference for a specific set of structures. Further analysis was performed by sequential permethylation, desulfation, and pertrideuteroacetylation followed by online separation and structural analysis by MS/MS. Sequences of tetrasaccharides could be deduced from the data, and by combining the compositional and sequence data, a putative octasaccharide ligand could be proposed (GlA-GlcNS6S-IdoA-GlcNS-IdoA2S-GlcNS6S-IdoA-GlcNAc6S). A modular synthetic approach was employed to prepare the target compound, and binding studies by surface plasmon resonance (SPR) confirmed it to be a high affinity ligand for Robo1. Further studies with a number of tetrasaccharides confirmed that sulfate esters at C-6 are critical for binding, whereas such functionalities at C-2 substantially reduce binding. High affinity ligands were able to reverse a reduction in endothelial cell migration induced by Slit2-Robo1 signaling.

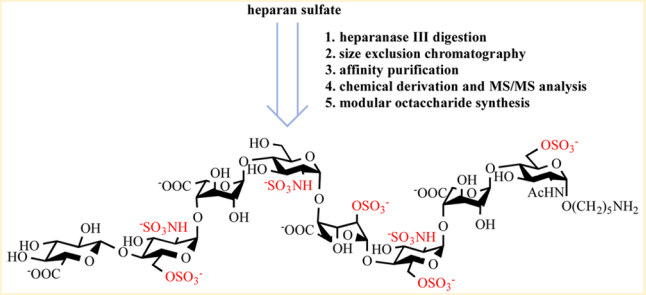

INTRODUCTION

Heparan sulfate (HS) is a highly complex and structurally diverse polysaccharide that is expressed by virtually all mammalian cell types.[1] The interaction between proteins and HS is critical for many biological processes including cell−cell and cell−matrix interactions, cell migration and proliferation, growth factor sequestration, chemokine and cytokine activation,[2] and tissue morphogenesis during embryonic development.[3] In addition, many pathogens including bacteria, viruses, and parasites attack host cells by binding to HS, which is often a decisive factor for infection.[4] There is data to support that HS encodes information within its chains by imparting an ability to selectively bind proteins, thereby regulating biological and disease processes.[1,5]

The biosynthesis of HS is initiated by the addition of a GlcNAc moiety to the tetrasaccharide GlcAβ1-3Galβ1-3Galβ1-4Xylβ1 that is linked to a serine residue of proteoglycan core proteins such as syndecans and glypicans.[5b] Chain elongation is carried out by members of the EXT gene family, which alternately add GlcNAc and GlcA residues. Discrete regions of the resulting heparosan polymer are then modified by *N*-deacetylase/*N*-sulfotransferases (NDSTs) to replace *N*-acetyl groups by *N*-sulfates. Next, regions of N-sulfation are further modified by a C-5 epimerase, which converts GlcA to IdoA, which is followed by O-sulfation by iduronosyl 2-*O*-sulfotransferase (HS2ST), glucosaminyl 6-*O*-sulfotransferases (HS6STs), and 3-*O*-sulfotransferases (HS3STs). At the cell surface, HS can be further remodeled by sulfatases that remove 6-*O*-sulfate esters and heparanases that cleave HS chains.[1]

HS modifications occur in distinct regions and are often incomplete resulting in at least 20 different HS-disaccharide

Received: August 5, 2016
Published: September 9, 2016

DOI: 10.1021/jacs.6b08161
J. Am. Chem. Soc. 2016, 138, 13059−13067

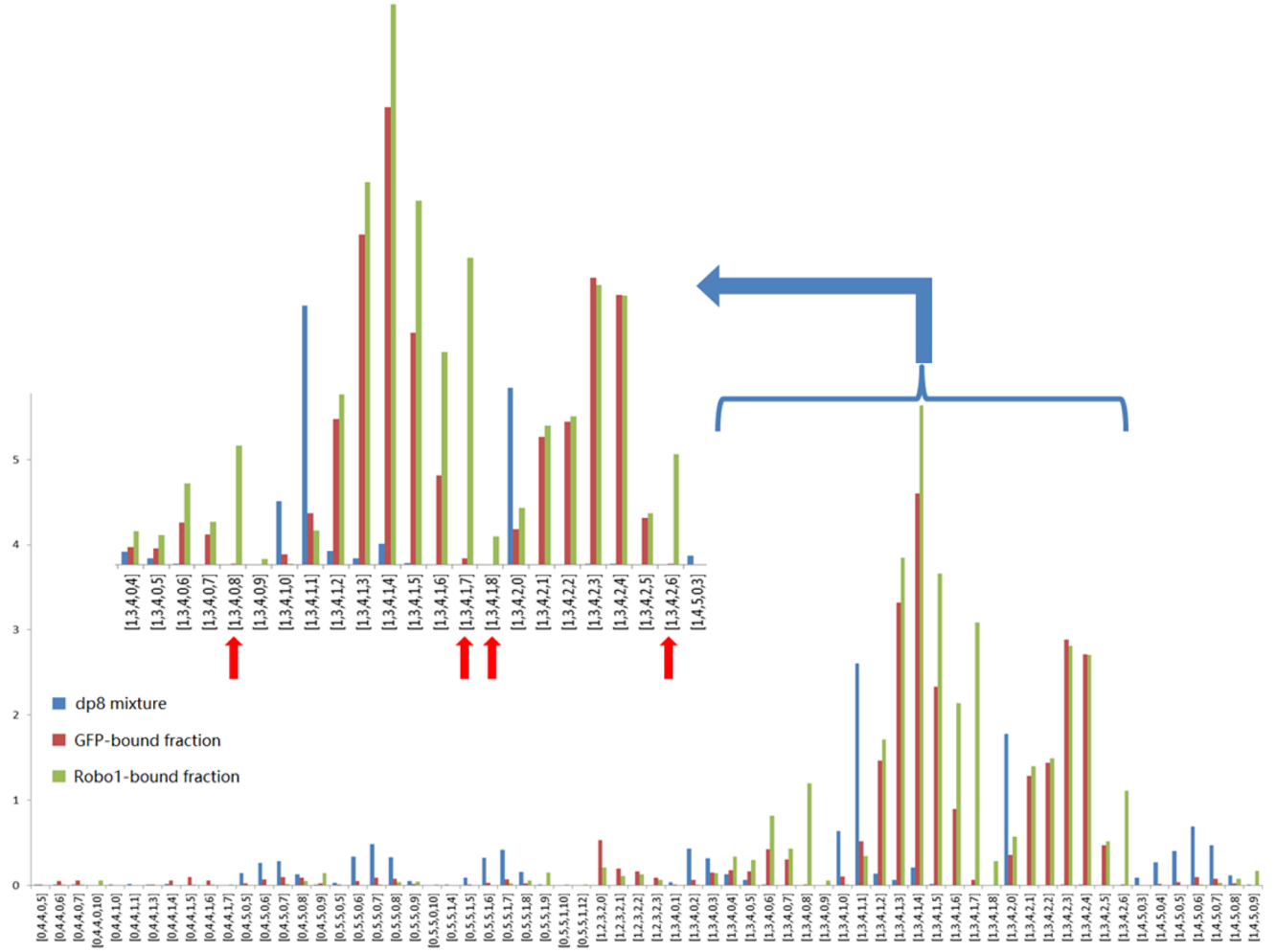

Figure 1. Composition analysis of the octasaccharide mixture, the GFP-bound fraction, and the Robo1-bound fraction. Each composition is given as follows: [ΔHexA, HexA, GlcN, Ac, SO_3]. Abundances are relative to the overall amount of HS detected in that sample and are not directly comparable between samples. Inset: An enlarged view of the region with the most abundant compositions; the four compositions only observed significantly in the Robo1-bound fraction are indicated by red arrows, with the largest amount of specific binding being detected for the composition [1,3,4,1,7].

moieties, which can be combined in different manners creating considerable structural diversity. Analyses of HS isolated from different mammalian tissues indicate the existence of tissue-specific compositions.[5a,6] Furthermore, immuno-histochemical analyses using antibodies that recognize specific HS-epitopes indicate that unique patterns of HS-motifs occur within tissues. Alteration in HS expression has been associated with disease,[7] and for example, significant changes in the composition of proteoglycans occur in the stroma surrounding tumors, which appear to support tumor growth and invasion. These observations support a model in which HS structural diversity is not random but regulated in a context-dependent manner. Such regulation may be a result of the selective expression of isoforms of enzymes, their substrate specificities, and formation of enzyme complexes.

Although there is support for the existence of a so-called "HS interactome",[8] ligand requirements of HS-binding proteins have been defined for only a few HS-binding proteins.[5c] The latter is due to lack of technologies that can readily and reliably determine ligand requirements of such proteins.[9] Here, we report an integrated methodology to determine ligand requirements for HS binding proteins based on a workflow in which (i) a mixture of HS octasaccharides is produced by partial enzymatic degradation of natural HS followed by size exclusion purification; (ii) affinity purification of HS-oligosaccharides uses a HS-binding protein of interest; (iii) putative structure determination of isolated compounds is done by a hydrophilic interaction chromatography–high-resolution mass spectrometry (HILIC–HRMS) platform, and (iv) chemical synthesis of well-defined HS oligosaccharides is performed for structure–activity relationship (SAR) studies.

The new integrated methodology was employed to determine ligand requirements for the HS-binding protein Roundabout receptor 1 (Robo1). In most tissues, control of cell migration and cell–cell interaction is of critical importance for the development of functional structures. Several families of secreted molecules have been implicated in regulating these development processes including the Slit proteins and their Robo receptors.[10] Initially, these proteins were implicated in axon guidance by providing repulsive cues during the assembly of the nervous system. Recent studies indicate that the Slit/Robo signaling is also involved in muscle precursor cell migration, leukocyte and hematopoietic stem cell trafficking, and development of lung, kidney, heart, and diaphragm.[11] They also play roles in disease processes such as inflammation, tumor metastasis, and angiogenesis.[12]

DOI: 10.1021/jacs.6b08161
J. Am. Chem. Soc. 2016, 138, 13059–13067

Table 1. Chemical Derivatization and Identification of Tetrasaccharide Sequences from the Chemically Derivatized HS-Octasaccharides in the Robo1-Bound Fraction

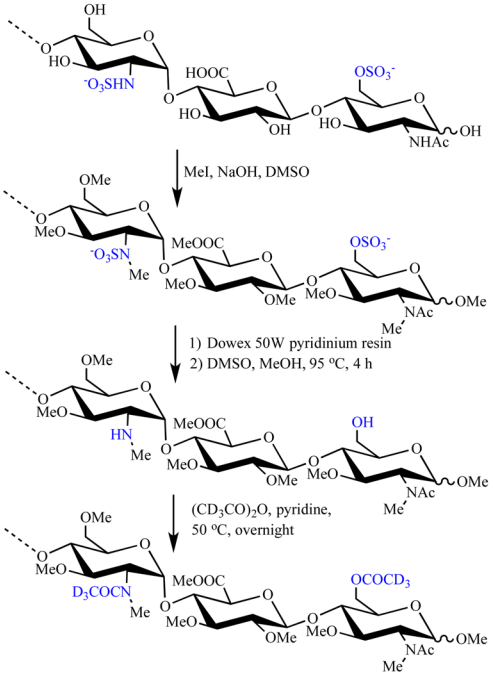

STRUCTURE	DB_MZ	Composition
HexA2S-GlcNAc6S-HexA-GlcNAc-ol	1057.469	[0,2,2,1,4]
d-HexA2S-GlcNS6S-HexA-GlcNAc6S-ol d-HexA2S-GlcNS6S-HexA2S-GlcNAc-ol d-HexA2S-GlcNAc6S-HexA2S-GlcNS-ol	1059.476	[1,1,2,1,4]
d-HexA2S-GlcNS6S-HexA-GlcNAc-ol d-HexA2S-GlcNAc6S-HexA-GlcNS-ol	1028.462	[1,1,2,1,3]
d-HexA-GlcNS3S-HexA2S-GlcNAc-ol d-HexA2S-GlcNS3S-HexA-GlcNAc-ol	1014.446	[1,1,2,1,3]
d-HexA-GlcNS6S-HexA-GlcNS-ol d-HexA2S-GlcNS-HexA-GlcNS-ol d-HexA-GlcNS-HexA2S-GlcNS-ol	1000.467	[1,1,2,0,3]
d-HexA-GlcNAc6S-HexA-GlcNS-ol d-HexA-GlcNS-HexA-GlcNAc6S-ol d-HexA-GlcNS-HexA2S-GlcNAc-ol d-HexA2S-GlcNS-HexA-GlcNAc-ol	997.448	[1,1,2,1,2]
d-HexA-GlcNAc6S-HexA-GlcNAc-ol	994.429	[1,1,2,2,1]
d-HexA-GlcNS3S-HexA-GlcNS-ol	986.451	[1,1,2,0,3]
d-HexA-GlcNS3S-HexA-GlcNAc-ol	983.433	[1,1,2,1,2]
d-HexA-GlcNS-HexA-GlcNS-ol	969.453	[1,1,2,0,2]
d-HexA-GlcNS-HexA-GlcNAc-ol d-HexA-GlcNAc-HexA-GlcNS-ol	966.434	[1,1,2,1,1]
d-HexA-GlcNAc-HexA-GlcNAc-ol	963.416	[1,1,2,2,0]
d-HexA-GlcNAc6S-HexA-GlcN-ol d-HexA2S-GlcNAc-HexA-GlcN-ol	958.468	[1,1,2,1,1]

Genetic and biological studies have shown that Slit/Robo function critically depends on HS as a coreceptor, and there are data that indicate that Slit/Robo/HS signaling involves the formation of a ternary complex.[10,13] While crystallographic studies and structure-based mutagenesis have identified residues of Robo involved in HS binding,[14] little is known about its ligand requirements. Surface plasmon resonance (SPR) analysis[13] using chemically modified heparin indicated that *N*-sulfo and 6-*O*-sulfo groups are important for HS−Robo1 interactions. Further exploration of the specific structure was impeded by the heterogeneity of HS and lack of *ex-vivo* tools.

RESULTS AND DISCUSSION

Affinity-Purified and Structural Identification of Bound HS-Octasaccharides. A mixture of natural HS oligosaccharides was prepared by partial enzymatic digestion of HS (Celsus Laboratories) with heparinase III followed by purification by size exclusion column chromatography using a Bio-Gel P-10 column. The starting material is resistant to heparinase I (specific to heparin), and therefore oligosaccharides were generated using heparinase III (specific to HS) to ensure generation of an oligosaccharide mixture with compositions consistent with HS.[15] Octosaccharides (dp8) were retrieved to identify compounds that can selectively bind to Robo1. It was anticipated that such oligosaccharides are structurally sufficiently diverse to contain potentially unusual epitopes yet not too large for structural analysis. Furthermore, for other HS binding proteins such as FGF2, dp8 oligosaccharides can recapitulate full biology by forming ternary complexes.[16] An affinity resin was prepared by binding of a biotinylated fusion protein of human Robo1 and GFP to a streptavidin−agarose column. Recently, it was shown that GFP can bind HS,[17] and therefore an additional affinity resin for HS depletion was prepared containing biotinylated GFP alone. First, the natural HS mixture was passed through the GFP depletion column in a low-salt buffer (0.15 M NH_4OAc, pH 7.4) to capture GFP-binding HS sequences, and the unbound flow-through and low-salt wash was collected. The bound compounds were released by employing a high-salt buffer (2 M NH_4OAc, pH 7.4). The unbound flow through was applied to the Robo1-GFP fusion affinity column, and the bound compounds were released by using the high-salt buffer. Compositional differences between the octasaccharides in the starting mixture and the GFP and Robo1-bound fractions were determined by HILIC−HRMS.[18] Analysis of the data using the software package GlycReSoft[19] gave four dp8 compositions, [1,3,4,0,8], [1,3,4,1,7], [1,3,4,1,8], and [1,3,4,2,6], that were highly enriched in the Robo1-bound fraction (Figure 1), indicating that Robo1 has a preference for a specific set of structures. The most enriched composition was [1,3,4,1,7] that was present as only a very minor component in the starting dp8 mixture and the GFP-bound fraction.

Although the compositional analysis provides useful information about the ligand requirements of Robo1, the identified compositions represent too large a number of isomeric compounds to guide chemical synthesis of putative ligands. Therefore, the Robo1-binding octasaccharides were further analyzed by sequential permethylation, desulfation, and pertrideuteroacetylation followed by online separation and structural analysis by MS/MS.[20] By replacing the polar and labile sulfates with much more stable and hydrophobic trideuteroacetyl groups, oligosaccharides were obtained that could be separated by reverse-phase capillary HPLC and fragmented by MS/MS without loss of information on sites of modification. The structural complexity of HS oligosaccharides increases exponentially as oligosaccharides become larger, and therefore manual interpretation of MS/MS spectra and identification of isomeric sequences is challenging. Therefore, an in-house developed program (GAG-ID) was used to facilitate data analysis with all final assignments performed manually.[21] An overview of the GAG-ID program is shown in the Supporting Information (Figures S1 and S2).

DOI: 10.1021/jacs.6b08161
J. Am. Chem. Soc. 2016, 138, 13059−13067

Scheme 1. Octasaccharide Synthesis[a]

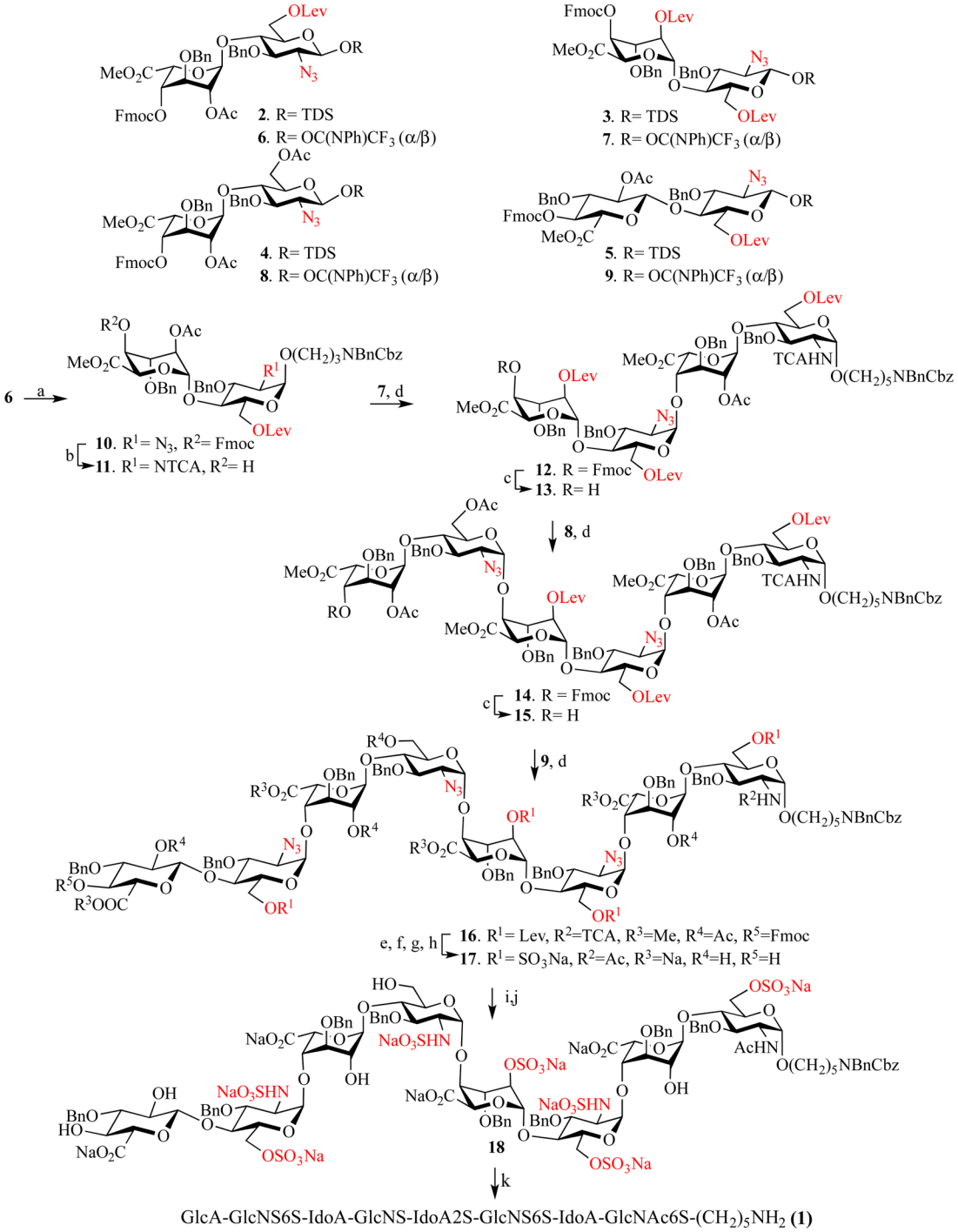

[a]Reagents and conditions: (a) TfOH, $HO(CH_2)_5NBnCbz$, toluene/dioxane (1/3, v/v), −30 °C, 56%; (b) (i) Zn, AcOH, DCM; (ii) TCACl, THF, $NaHCO_3$, then NEt_3, 70% over three steps; (c) Et_3N, DCM (**13**, 89%; **15**, 74%); (d) TfOH, DCM, −30 °C (**12**, 54%; **14**, 56%; **16**, 53%); (e) NH_2NH_2 AcOH, DCM/MeOH; (f) SO_3Pyr., DMF; (g) H_2O_2, LiOH, NaOH, THF, 48 h; (h) Ac_2O, Et_3N, MeOH, 26% over four steps; (i) PMe_3, THF, NaOH aq; (j) SO_3Pyr., THF, Et_3N, NaOH, 72 h, 50% for two steps; (k) $Pd(OH)_2$/C, H_2, pH = 7.4 phosphate buffer, 48 h, 68%.

No specific oligosaccharide sequences of any length could be identified with confidence from the GFP-bound fraction, probably due to a lack of specificity for binding any particular structures. Also, no sequences could be identified with confidence in the theoretical dp8 or dp6 databases, and no specific dp8 or dp6 sequences were seen by manual analysis of the Robo1-bound fraction. Confident identifications could, however, be made when the data were searched against a comprehensive dp4 database to give 24 manually verified tetrasaccharides as top hits spread across 13 compositions (Table 1). A representative example of an identified partial sequence is shown in Figure S3. Previous studies using synthetic oligosaccharide standards have shown that *β*-elimination can occur during the permethylation step, generating shorter sequences.[20a] The generated tetrasaccharides

DOI: 10.1021/jacs.6b08161
J. Am. Chem. Soc. 2016, 138, 13059−13067

represent partial sequences of the original octasaccharides, which are valuable for structure identification.

At least 256 tetrasaccharide sequences (not considering uronic acid epimerization) are possible, and only a small subset was observed in the Robo1 affinity purified material. The identified partial sequences revealed very few $GlcNH_2$ (GlcN) residues and none with more than one GlcN in a tetrasaccharide sequence. Sulfation was generally much higher in the partial sequences than in the starting material, with all sulfation sites represented in at least one partial sequence, including the rare 3-*O*-sulfation of GlcNS. The vast majority of the partial sequences contained at least one GlcNS. Contrary to the canonical repetitive domain structure often represented to dominate GAG sequences, most of the partial sequences identified contained nonrepetitive structures. Because of the overlapping enrichment of the moderately sulfated octasaccharides on the Robo-GFP fusion column compared with the GFP depletion column, we focused on partial sequences that could be derived from the highly sulfated compositions that were preferentially enriched only on the Robo1-GFP column.

A putative octasaccharide ligand for Robo1 was proposed by combining two identified tetrasaccharides to give octasaccharide compositions equivalent to those that were identified by the LC−MS compositional analysis to bind specifically to Robo1 and not to GFP (Figure 1). The combination of the dp4 compositions [1,1,2,1,4] and [1,1,2,0,3] gives dp8 composition [1,3,4,1,7], which was highly enriched in the Robo1-bound fraction. The tetrasaccharide sequences d-HexA2S-GlcNS6S-HexA-GlcNAc6S-ol and d-HexA-GlcNS6S-HexA-GlcNS-ol were chosen from dp4 compositions [1,1,2,1,4] and [1,1,2,0,3] due to their high ion intensity in the LC−MS/MS spectra. The internal HexA residue of the two tetrasaccharides was assigned as IdoA due to the observed Z_2/Y_2 ratio of ∼0.3 (Figure S4). In this respect, previous studies have shown that a Z_2/Y_2 ratio of ∼0.3 of tetrasaccharides is indicative of IdoA, while a Z_2/Y_2 ratio of ∼0.9 is indicative of GlcA.[20b]

Due to unsaturation at the nonreducing end that occurs during the lyase cleavage, the nature of the central uronic acid in the intact octasaccharide cannot be determined based on MS/MS data. However, IdoA is much more likely to be modified by 2-O-sulfation than GlcA, and therefore the internal HexA2S residue was assigned as IdoA2S. Based on this rationale, we propose d-HexA-GlcNS6S-IdoA-GlcNS-IdoA2S-GlcNS6S-IdoA-GlcNAc6S as a potential ligand for Robo1. The dHexA at the nonreducing end of the octasaccharide was assigned as GlcA for synthesis because heparinase III has a strong preference for cleaving at this uronate. It is important to note that the compositional and sequencing data indicate that not one unique but a range of related octasaccharides may bind with high affinity to Robo1. However, it is likely that the identified sequence contains structural elements important for binding.

Chemical Synthesis of the Octasaccharide GlcA-GlcNS6S-IdoA-GlcNS-IdoA2S-GlcNS6S-IdoA-GlcNAc6S. To validate whether the proposed octasaccharide is a ligand for Robo1, compound **1** was chemically synthesized for binding and biological studies. A number of tetrasaccharides were also prepared to determine which features of the octasaccharide are important for binding and biological activity.

Several laboratories have successfully prepared relatively large HS-oligosaccharides.[22] These approaches are, however, mainly focused on the preparation of compounds composed of the same repeating unit and therefore are less suited to prepare HS oligosaccharides for SAR studies. We are developing a modular approach for HS oligosaccharide synthesis that uses a set of building blocks that resemble the differently sulfated disaccharides found in HS.[22c,23] These compounds can easily be converted into glycosyl donors and acceptors for rapid oligosaccharide assembly. The disaccharide building blocks are modified by selectively removable levulinoyl esters (Lev)[24] at positions where eventually sulfates need to be installed (Scheme 1). The anomeric center is protected as a TDS ether and the C-4′ hydroxyl as an Fmoc carbamate. Selective removal of the latter protecting groups can give easy entry into glycosyl donors and acceptors for oligosaccharide assembly. A limitation of the methodology is that it does not allow the introduction of an acetamido and *N*-sulfate in one compound. The latter is due to the use of azido functions, which mask the amino groups and are required for introducing α-glycosidic linkages. At the end of a synthetic sequence, the azido groups are reduced and either acetylated or sulfated. To differentiate N-substitutions, the tricholoroacetyl group (TCA) was employed to protect the amine that at the end of the synthetic sequence needs to be converted into an acetamido moiety. To allow the installation of an α-glycosidic linkage, the TCA was introduced in a postglycosylation manner by reducing an azide to an amine followed by tricholoroacetylation.

The targeted octasaccharide **1** was assembled from modular disaccharides **2**, **3**, **4**, and **5**,[22c] which could easily be converted into glycosyl donors **6**, **7**, **8**, and **9** using standard manipulations (Scheme 1). Thus, a triflic acid mediated glycosylation of **6** with 5-amino-1-pentanol protected with *N*-benzyloxycarbonate and *N*-benzyl groups gave spacer-modified **10** in a yield of 56% as a separable mixture of α/β glycosides (α/β = 3/1). The azido moiety of **10** was reduced by treatment with zinc and acetic acid in dichoromethane to give an amine, which was protected as a trichloroacetamide by reaction with trichloroacetyl chloride (TCACl) in THF in the presence of sodium bicarbonate. The Fmoc-protecting group was removed *in situ* by the addition of Et_3N to the reaction mixture to give glycosyl acceptor **11**. The latter compound was coupled with glycosyl donor **7** in the presence of triflic acid as the activator to afford tetrasaccharide **12** as only the α-anomer in a yield of 54%. The modest yield was attributed to the presence of the protected aminopentyl linker, which in our experience lowers yields of glycosylations. Furthermore, uronic acids are notoriously poor glycosyl acceptors,[25] which is attenuated by the electron-withdrawing groups at C-2 and C-6 of acceptor **11**. The process of Fmoc removal and glycosylation was repeated twice by employing glycosyl donors **8** and **9** to give fully protected octasaccharide **16**. In each glycosylation only the α-anomer was observed.

The selective conversion of the TCA function into an acetamido group was a critical step for the preparation of **1**. This transformation is often performed by treatment with a zinc/copper couple in acetic acid;[26] however, in the case of compound **16** this procedure gave a low yield of product. Therefore, we explored an alternative strategy in which at a late stage of modification all base labile protecting groups including the TCA function are removed by base treatment followed by selective N-acetylation and then reduction of the azides to amines, which can then be selectively sulfated. Thus, the Lev esters of **16** were selectively removed by treatment with hydrazine acetate to give hydroxyls that were sulfated with pyridinium trisulfate in DMF. The resulting compound was treated with a mixture of H_2O_2 and LiOH and then aq. NaOH in THF to saponify all esters and remove the TCA group. The

DOI: 10.1021/jacs.6b08161
J. Am. Chem. Soc. 2016, 138, 13059−13067

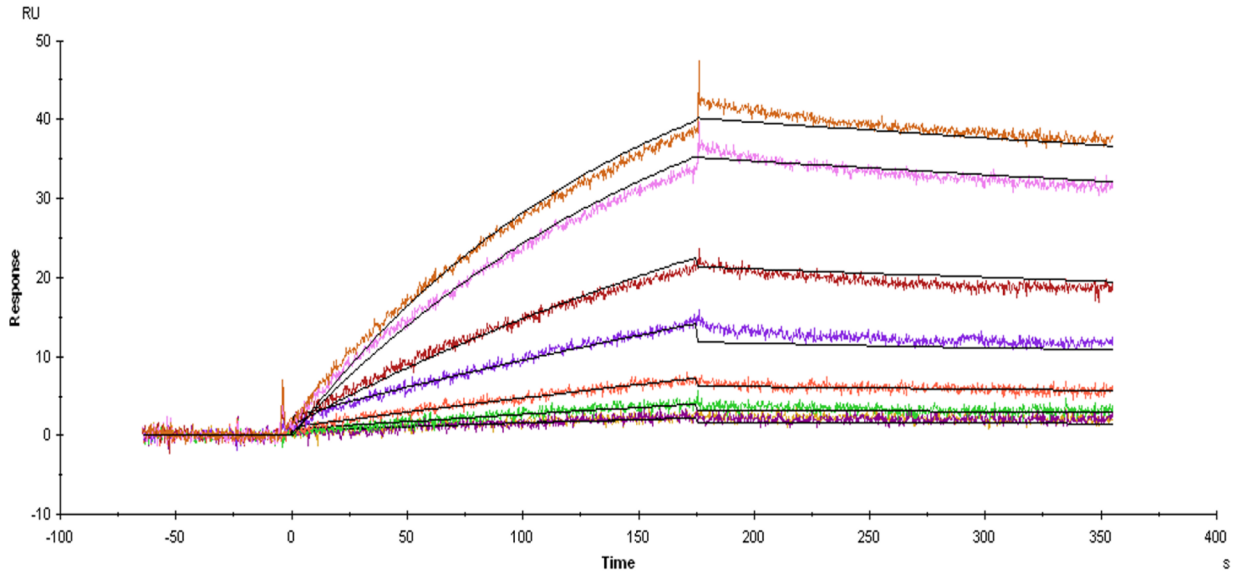

Figure 3. SPR sensorgram representing the concentration-dependent kinetic analysis of the binding of **1** with immobilized Robo1 on a CM5 chip. Concentration of compound **1** (from top to bottom): 100, 80, 40, 20, 10, 5, and 2.5 μM, fitted with a Langmuir 1:1 binding model (black lines).

resulting octasaccharide was treated with acetic anhydride and triethyl amine in methanol to give partially modified octasaccharide **17**. The azido functions of **17** were reduction by Staudinger reaction using PMe_3, and the resulting amines were N-sulfated employing pyridinium sulfate in THF in the presence of Et_3N and NaOH to give compound **18**. The N-sulfation took a rather longer time probably due to steric hindrance. The final deprotection step entailed hydrogenation over $Pd(OH)_2/C$ in phosphate buffer to give, after purification by P2 size exclusion column chromatography, compound **1**. Two-dimensional NMR experiments combined with high-resolution ESI-MS confirmed the structural integrity of the compound. The J_{H-H} coupling constants of seven anomeric protons were between 3 and 4 Hz, indicating α-glycosidic linkages, while the coupling constant of an anomeric proton at 4.46 ppm is 7.8 Hz indicating a β-glycosidic linkage for the nonreducing glucuronic acid. Sites of sulfate esters were identified by downfield shifts of ring protons (~0.4 ppm) and carbons (~4 ppm). The H2 of *N*-acetyl glucosamine was down shifted by 0.66 ppm compared with that of N-sulfated glucosamines.

Binding and Biological Studies. Binding studies were performed by surface plasmon resonance (SPR) to validate that compound **1** is a high affinity ligand for Robo1. Recombinant Robo1 was immobilized on a CM5 sensor chip surface having NHS-activated carboxylic acid, and titration experiments were performed with the synthetic octasaccharide. The titration curves fit well to a Langmuir 1:1 binding mode, and a K_D value of 4.8 μM (Figure 3) was determined, which is comparable to the previously reported binding to porcine intestinal heparin (16 kDa, Langmuir 1:1 binding mode, K_D value 0.65 μM).[13]

Six tetrasaccharides were synthesized to further study the ligand requirements of Robo1. SPR measurements for IdoA-GlcNS6S-IdoA-GlcNS6S (**19**) gave a K_D value of ~20 μM. Interestingly, two other tetrasaccharides that have the same backbone but additional 2-*O*-sulfate ester(s) (IdoA-GlcNS6S-IdoA2S-GlcNS6S, **20**, and IdoA2S-GlcNS6S-IdoA2S-GlcNS6S, **21**) exhibited much reduced binding (see Table S1 and Figure S5). These studies indicate that 2-O-sulfation substantially reduces the binding of Robo1.

Cell Migration Studies. Slit2 is a cognate ligand of Robo1, and the Slit2−Robo1 signaling pathway participates in regulation of neuronal cell migration in development and endothelial cell migration in angiogenesis.[11b,27] Cell surface HS enhances Slit2−Robo1 interaction, thereby facilitating signaling pathway activation.[11a,14a] Using a Boyden-chamber endothelial cell migration system, we recently determined the regulatory function of HS in Slit3−Robo4-mediated endothelial cell migration.[11b] In the same assay system, supplementation of Slit2 in the bottom chamber lowered the number of the endothelial cells that had migrated from the upper chamber to the lower chamber, indicating that Slit2−Robo1 signaling acts as a repulsive signal to prevent endothelial cell migration in this assay. To determine if the deduced Robo1 binding HS structures modulate Slit2−Robo1 signaling in a cellular context, the Robo1-binding octasaccharide (**1**), the Robo1-binding tetrasaccharide IdoA-GlcNS6S-IdoA-GlcNS6S (**19**), and the non-Robo1-binding tetrasaccharide IdoA-GlcNS6S-IdoA2S-GlcNS6S (**20**) were tested by cosupplementing with Slit2 in the lower chamber in the assay (Figure 4). The addition of the Robo1-binding oligosaccharides **1** and **19**, but not the non-Robo1-binding oligosaccharide **20**, increased the number of endothelial cells that migrated into the lower chamber side, showing that the added Robo1-binding oligosaccharides inhibited Slit2−Robo1 signaling in the assay. This observation suggests that mechanistically the synthesized Robo1-binding HS oligosaccharides compete with cell surface HS to disturb cell surface Slit2−Robo1−HS ternary complex formation, thereby inhibiting Slit2−Robo1 signaling.

■ CONCLUSION

Due to the complexity of HS and sequencing method limitations, identification of high affinity ligands for HS-binding proteins remains very challenging. We identified a putative ligand for Robo1 by affinity enrichment of a mixture of natural octasaccharide followed by compositional analysis by MS/MS and sequence determination by sequential permethylation, desulfation, and pertrideuteroacetylation followed by online separation and structural analysis by MS/MS. The sequencing method did not reveal any octasaccharide structures, probably

DOI: 10.1021/jacs.6b08161
J. Am. Chem. Soc. 2016, 138, 13059−13067

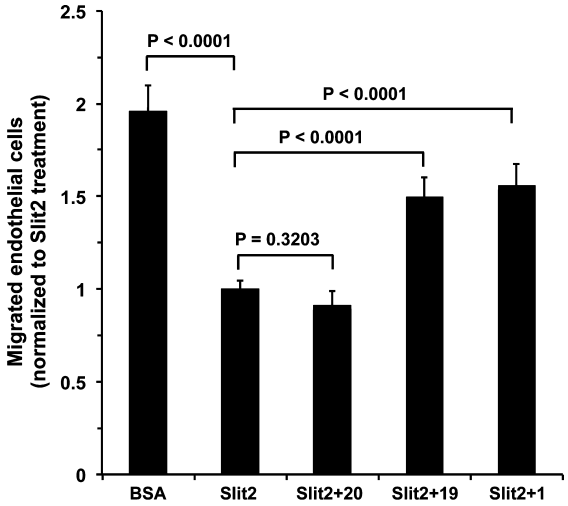

Figure 4. Robo1-binding octa- and tetrasaccharides reverted the inhibition of Slit2−Robo1 signaling on mouse diaphragm endothelial cell migration. Serum-starved immortalized mouse lung endothelial cells in serum-free medium were seeded into the upper chamber of a RTCA CIM-16 plate (ACEA Biosciences). Slit2 (1 μg/mL) without or with oligosaccharide (50 μg/mL) was supplemented in serum-free medium in the lower chamber. Bovine serum albumin (BSA) was included as a negative control of Slit2. The cell migration to the lower side of the chamber membrane was monitored by a RTCA DP plate reader (ACEA Biosciences). Statistical analysis was carried out using two-tailed Student *t* test.

due to β-elimination during the base-mediated permethylation step, resulting in smaller fragments. Alternative methylation conditions need to be developed that do not require strong basic conditions so that the large HS fragments stay intact. The analysis did, however, uncover structures of tetrasaccharides, which represent partial sequences of the original octasaccharides, and a putative sequence could be deduced by combining the compositional data with the identified tetrasaccharide sequences. The identified octasaccharide is mainly sulfated at the C-6 position and contained only one C-2 sulfate ester. Disaccharides that have only a sulfate ester at C-6 are relatively rare in heparan sulfate, and the identified octasaccharide contains multiple of such motifs indicating that a rare sequence had been identified. The octasaccharide was prepared by a modular approach in which properly protected disaccharide donors, which resemble the differently sulfated structures found in HS, can be assembled into complex structures. The trichloroacetyl group was employed for postglycosylation modification of amines that at a late stage of synthesis needed to be converted into acetamido functions. Azides were used as masking groups for those amines that eventually need to be converted into *N*-sulfate derivatives. Binding studies using SPR confirmed that the octasaccharide is a good ligand for Robo1. Further binding studies with a series of tetrasaccharides confirmed that 6-*O*-sulfate esters are important for binding, whereas such functionalities at C-2 are not well tolerated by the protein. An interesting observation is, however, that the identified octasaccharide and a number of partial tetrasaccharide sequences (Table S1) contain a 2-*O*-sulfate ester. It is likely that the distal part of the octasaccharide, which does not contain a 2-*O*-sulfate ester, interacts with the main binding site of Robo1, and the proximal part that does contain such a moiety makes peripheral interactions with the proteins. Future structural studies will need to confirm the molecular basis of the binding of Robo1 with the octa- and tetrasaccharides.

Cell biology experiments confirmed that biologically relevant HS oligosaccharides have been identified. In this respect, it was found that Slit2−Robo1 signaling acts as a repulsive signal to prevent endothelial cell migration. Compounds that bind with relatively high affinity to Robo1 could block a reduction in Slit-mediated cell migration. It has been shown that relatively short HS-oligosaccharides such as tetrasaccharides can block FGF2/FGFR-mediated cell signaling, whereas longer oligosaccharides such as octasaccharides are activators.[16] For Slit2−Robo1, it appears that both tetra- and octasaccharides block cellular activation. It is important to note that both Robo1 and Slit can bind to heparan sulfate, and it cannot be excluded that the synthetic compounds differentially interact with these proteins.

EXPERIMENTAL SECTION

Materials. Green fluorescent protein (GFP)-tagged human Robo1 (IG domains 1 and 2), termed Robo1-GFP, was prepared as previously described.[13] Porcine intestinal heparan sulfate was purchased from Celsus Laboratories (Cincinnati, OH). Heparinase III was purchased from IBEX Technologies Inc. (Quebec, Canada). Gel filtration columns and packing materials were purchased from Bio-Rad (Hercules, CA) and packed as instructed by the manufacturer.

General Procedure for Glycosylation. Donor (1.2 equiv) and acceptor (1.0 equiv) were coevaporated with toluene (3 × 3 mL) and then dissolved in anhydrous DCM or toluene/dioxane (1/3, v/v) to maintain a concentration of 0.05 M. Freshly activated powdered 4 Å molecular sieves were added, and the mixture was stirred for 30 min at ambient temperature and then cooled to −20 °C. After adding TfOH (1 equiv), the reaction mixture was stirred for 1 h and then quenched by the addition of pyridine (5 μL). The mixture was filtered; the filtrate was concentrated under reduced pressure; and the residue was purified by silica gel column chromatography using a gradient of toluene and EtOAc (from 60/40 to 40/60, v/v) to give pure compound.

General Procedure for Fmoc Removal. The mixture of fully protected oligosaccharide in Et_3N and DCM (20/80, v/v) was stirred for 2 h until TLC indicated completion. Then the mixture was concentrated under reduced pressure, and the residue was purified by silica gel column chromatography using a gradient of hexanes and EtOAc (from 60/40 to 40/60, v/v) to give the according acceptor.

Generation of a Mixture of HS Octasaccharides. A mixture of HS octasaccharides was prepared by partial enzymatic digestion of intact HS, followed by gel filtration purification. Briefly, 100 mg of HS and 0.05 IU heparinase III were mixed in 1.5 mL buffer of 50 mM sodium acetate and 0.4 mM calcium acetate. The solution was incubated at 37 °C for a total of 48 h, with an additional aliquot of 0.05 IU heparinase III added after 24 h incubation. The enzyme digestion was stopped by heating the solution at 100 °C for 10 min. The depolymerized samples were subjected to gel filtration chromatography on a Bio-Gel P-10 column (2.5 × 100 cm) using 10% ethanol solution containing 1 M NaCl as a mobile phase to obtain octasaccharide fractions, which was further desalted through a Sephadex G-15 column (2.5 × 50 cm) and dried under vacuum.

Affinity Purification of HS Octasaccharides. Robo1-GFP or GFP were biotinylated by biotin-protein ligase (Avidity LLC, Aurora, CO) based on the manufacturer's protocol. Robo1-GFP-biotin was bound at 3.2 mg/mL on streptavidin-agarose resin (Thermo Scientific Pierce, Rockford, IL). GFP-biotin was bound at 1.6 mg/mL on streptavidin-agarose resin. Each resin (1 mL) was poured into empty plastic columns and equilibrated in 0.15 M ammonium acetate buffer (pH 7.4), designated as Robo1-GFP column and GFP column, respectively.

A mixture of HS octasaccharide (0.7−0.8 mg) in 1 mL of 0.15 M ammonium acetate buffer was loaded to the GFP column, and the column was capped and rotated at room temperature (RT) for 2 h. After incubation, the flow-through fraction was collected and pooled

DOI: 10.1021/jacs.6b08161
J. Am. Chem. Soc. 2016, 138, 13059−13067

with a wash of 3 mL of 0.15 M ammonium acetate (with final volume of approximately 4 mL). The column was further washed by an additional 10 mL of 0.15 M ammonium acetate. The bound HS octasaccharides were eluted and collected in 8 mL of 2.0 M ammonium acetate, being designated as *GFP-bound fraction*. The collected flow-through and wash fraction in 4 mL of 0.15 M ammonium acetate was loaded to the Robo1-GFP column and rotated at RT for 2 h. After incubation, the column was extensively washed by 10 mL of 0.15 M ammonium acetate. The bound HS octasaccharides were eluted and collected in 8 mL of 2.0 M ammonium acetated, being designated as *Robo1-bound fraction*.

Hydrophilic Interaction Chromatography–High-Resolution Mass Spectrometry. The HS octasaccharide mixture (referred to as dp8 mixture), the GFP-bound fraction, and Robo1-bound fraction were subjected to hydrophilic interaction chromatography–high-resolution mass spectrometry (HILIC–HRMS) for composition analysis.[18] HILIC–HRMS was performed on a Thermo LTQ Orbitrap XL instrument coupled with Surveyor HPLC System (Waltham, MA). A homemade spray tip (0.08 × 130 mm) packed with amide-80 material (3 μm, TOSOH Biosciences) to 110 mm long was used for LC separation. Buffer A was 80% 55 mM ammonium formate in water (pH 4.4), and buffer B was prepared as 95% acetonitrile and 5% buffer A. A linear gradient of 65 to 30% buffer B over 30 min was used, with a flow rate of 135 μL/min per set for the pump delivering an actual column flow rate between 0.3 and 0.4 μL/min after splitting. MS analysis was performed in the Orbitrap analyzer in negative ion mode. The dp8 mixture (5 μg), GFP-bound fraction (estimated 5 μg), and Robo1-bound fraction (estimated 5 μg) were suspended in 50 μL of 65% buffer B, and 10 μL was loaded onto the amide-80 packed tip for LC/MS analysis. LC/MS data were analyzed by GlycResoft[19] following deconvolution using DeconTools (open source software available at http://omics.pnl.gov/software/DeconTools.php).

Chemical Derivatization of Robo1-Bound HS Octasaccharides. The Robo1-bound fractions from the dp8 mixture were subjected to the chemical derivatization protocol as described previously.[20a] Briefly, the HS octasaccharides were first converted into their triethylammonium (TEA) salt form and lyophilized. The dried HS octasaccharide TEA salts were permethylated using sodium hydroxide and methyl iodide in dimethyl sulfoxide (DMSO), followed by desalting using a C18 Sep-Pak cartridge (Waters Co.) and conversion to pyridinium salts. The pyridinium salts of the permethylated products were resuspended in DMSO containing 10% methanol and incubated for 4 h at 95 °C to remove the sulfate groups. The dried desulfated products were then trideuteroacetylated by incubating with D_6-acetic anhydride in pyridine at 50 °C overnight, and solvent was dried under vacuum.

LC-MS/MS Analysis. Online LC separation of derivatized octasaccharides was performed on a Thermo Finnigan Surveyor HPLC System, using a homemade spray tip (0.08 × 130 mm) packed with C18 resin (5 μm, 300 Å, Mettler-Toledo, LLC) to 110 mm long. Buffer A was 0.1% formic acid in water with 1 mM sodium acetate, and buffer B was prepared as 80% acetonitrile/water with 0.1% formic acid and 1 mM sodium acetate. A linear gradient of 20%–100% buffer B over 80 min was used, with a flow rate of 135 μL/min set for the pump delivering an actual column flow rate between 0.3 and 0.4 μL/min after splitting. The derivatized Robo1-bound HS octasaccharides were suspended in 10 μL of 20% buffer B, and 5 μL was loaded onto the C18-packed tip for LC-MS/MS analysis.

Mass spectrometry was performed on a Thermo LTQ Orbitrap XL instrument (Waltham, MA). Both full MS and CID-MS/MS spectra were acquired by Orbitrap in positive ion mode. A data-dependent MS/MS method was used, with the top six abundant precursor ions selected, to trigger CID-MS/MS fragmentation. Instrument parameters were set as spray voltage at 1–2 kV, capillary voltage at 40 V, tube lens at 80 V, and capillary temperature at 250 °C. The collision energy for CID fragmentation was set at 40 V.

Automatic Sequencing by GAG-ID. An automatic sequencing program, GAG-ID (Figure S1), has been developed in our lab for the chemical derivatization based LC-MS/MS structural analysis of heparin/HS oligosaccharides, which use a database specifically designed for derivatized heparin/HS oligosaccharides (Figure S2). A theoretical database for oligosaccharides with different lengths can be generated as illustrated in Figure S2A, with theoretical mass for each residue listed in Figure S2B. Both saturated and unsaturated nonreducing ends are considered, while the reducing end can be either reduced or nonreduced before the sequential derivatizations (permethylation, desulfation, and trideutero-acetylation). For a glucosamine residue, the relatively rare 3-O-sulfation is also considered in addition to regular modifications, which presents as GlcNS3S or GlcNS3S6S in the current version of GAG-ID. Sequential glycosidic-bond cleavage fragments, B, Y, C, and Z ions (as illustrated in Figure S2C), as well as commonly observed neutral losses for derivatized GAGs, are also calculated to generate theoretical fragment lists. Each isomeric sequence under the same mass entry has its own fragment list, which can be used to match against the experimental MS/MS peak list, and a score would be calculated based on the number and relative intensity of the matched product ions.

SPR Binding Experiments. The binding interaction between different compounds and Robo1 was examined by SPR using a Biacore T100 instrument (Biacore Inc., GE Healthcare, USA). Robo1 was immobilized on a CM5 sensor chip (Biacore Inc., GE Healthcare) by standard amine coupling using an amine coupling kit. The surface was activated using freshly mixed *N*-hydroxysuccimide (NHS; 100 mM) and 1-(3-(dimethylamino)propyl)-ethylcarbodiimide (EDC; 391 mM) (1/1, v/v) in water. Next, Robo1 (100 μg/mL) in aqueous NaOAc (10 mM, pH 5.0) was passed over the chip surface until a ligand density of approximately 2800 RU was achieved. The remaining active esters were quenched by aqueous ethanolamine (1.0 M, pH 8.5). The control flow cell was activated with NHS and EDC followed by immediate quenching with ethanolamine. HBS-EP (0.01 M HEPES, 150 mM NaCl, 3 mM EDTA, 0.005% polysorbate 20; pH 7.4) was used as the running buffer for the immobilization and kinetic studies. A serial dilution of each compound in HBS-EP buffer and a 30 μL/min flow rate were employed for association and dissociation at a constant temperature of 25 °C. The surface was regenerated by a 30 s injection of aqueous NaCl (2.0M) at a flow rate of 30 μL/min. Data were fitted to a 1:1 binding model using BIAcore T100 evaluation software to obtain the equilibrium constant (K_D) data.

Cell Migration Assay. 80–90% confluent immortalized mouse diaphragmatic endothelial cells were starved for 9 h in DMEM. Then 20 000 cells were loaded to each well of a RTCA CIM-16 plate (ACEA Biosciences), and cell migration was monitored by a RTCA DP plate reader (ACEA Biosciences). Both top and bottom chambers contain DMEM (no serum added). In the bottom chamber, 1 μg/mL of BSA or Slit2 and/or 50 μg/mL indicated saccharides were added.

■ ASSOCIATED CONTENT

Supporting Information

The Supporting Information is available free of charge on the ACS Publications website at DOI: 10.1021/jacs.6b08161.

Figures S1–S5, Table S1, chemical synthesis and copies of NMR spectra (PDF)

■ AUTHOR INFORMATION

Corresponding Author

*gjboons@ccrc.uga.edu

Present Address

⊥Department of BioMolecular Sciences, University of Mississippi, University, MS, 38677, USA.

Notes

The authors declare no competing financial interest.

■ ACKNOWLEDGMENTS

This research was supported by the National Institute of General Medicine (NIGMS) of the National Institutes of Health (NIH) (Research Resource for Integrated Glycotech-

DOI: 10.1021/jacs.6b08161
J. Am. Chem. Soc. 2016, 138, 13059–13067

nology, P41GM103390). We thank Dr. John Glushka for technical assistance with NMR measurements and Dr. Joseph Zaia for technical support with the use of GlycResoft.

REFERENCES

(1) Bishop, J. R.; Schuksz, M.; Esko, J. D. *Nature* **2007**, *446*, 1030−1037.
(2) Lortat-Jacob, H. *Curr. Opin. Struct. Biol.* **2009**, *19*, 543−548.
(3) (a) Hacker, U.; Nybakken, K.; Perrimon, N. *Nat. Rev. Mol. Cell Biol.* **2005**, *6*, 530−541. (b) Kirn-Safran, C.; Farach-Carson, M. C.; Carson, D. D. *Cell. Mol. Life Sci.* **2009**, *66*, 3421−3434. (c) Kraushaar, D. C.; Dalton, S.; Wang, L. *Biol. Chem.* **2013**, *394*, 741−751.
(4) (a) Kamhi, E.; Joo, E. J.; Dordick, J. S.; Linhardt, R. J. *Biol. Rev. Camb. Philos. Soc.* **2013**, *88*, 928−943. (b) Garcia, B.; Merayo-Lloves, J.; Martin, C.; Alcalde, I.; Quiros, L. M.; Vazquez, F. *Front. Microbiol.* **2016**, *7*, 220.
(5) (a) Esko, J. D.; Lindahl, U. *J. Clin. Invest.* **2001**, *108*, 169−173. (b) Kreuger, J.; Kjellen, L. *J. Histochem. Cytochem.* **2012**, *60*, 898−907. (c) Xu, D.; Esko, J. D. *Annu. Rev. Biochem.* **2014**, *83*, 129−157.
(6) (a) van Kuppevelt, T. H.; Dennissen, M.; van Venrooij, W. J.; Hoet, R. M. A.; Veerkamp, J. H. *J. Biol. Chem.* **1998**, *273*, 12960−12966. (b) Lawrence, R.; Olson, S. K.; Steele, R. E.; Wang, L.; Warrior, R.; Cummings, R. D.; Esko, J. D. *J. Biol. Chem.* **2008**, *283*, 33674−33684.
(7) (a) Lindahl, U.; Kjellen, L. *J. Intern. Med.* **2013**, *273*, 555−571. (b) Vlodavsky, I.; Iozzo, R. V.; Sanderson, R. D. *Matrix Biol.* **2013**, *32*, 220−222.
(8) (a) Ori, A.; Wilkinson, M. C.; Fernig, D. G. *J. Biol. Chem.* **2011**, *286*, 19892−19904. (b) Pomin, V. H.; Mulloy, B. *Curr. Opin. Struct. Biol.* **2015**, *34*, 17−25.
(9) (a) Capila, I.; Linhardt, R. J. *Angew. Chem., Int. Ed.* **2002**, *41*, 390−412. (b) Powell, A. K.; Yates, E. A.; Fernig, D. G.; Turnbull, J. E. *Glycobiology* **2004**, *14*, 17−30. (c) Yates, E. A.; Rudd, T. R. *Int. J. Cardiol.* **2016**, *212*, S5−S9.
(10) Inatani, M.; Irie, F.; Plump, A. S.; Tessier-Lavigne, M.; Yamaguchi, Y. *Science* **2003**, *302*, 1044−1046.
(11) (a) Hu, H. *Nat. Neurosci.* **2001**, *4*, 695−701. (b) Zhang, B.; Xiao, W.; Qiu, H.; Zhang, F.; Moniz, H. A.; Jaworski, A.; Condac, E.; Gutierrez-Sanchez, G.; Heiss, C.; Clugston, R. D.; Azadi, P.; Greer, J. J.; Bergmann, C.; Moremen, K. W.; Li, D.; Linhardt, R. J.; Esko, J. D.; Wang, L. *J. Clin. Invest.* **2014**, *124*, 209−221.
(12) Mehlen, P.; Delloye-Bourgeois, C.; Chedotal, A. *Nat. Rev. Cancer* **2011**, *11*, 188−197.
(13) Zhang, F.; Moniz, H. A.; Walcott, B.; Moremen, K. W.; Linhardt, R. J.; Wang, L. *Biochimie* **2013**, *95*, 2345−2353.
(14) (a) Fukuhara, N.; Howitt, J. A.; Hussain, S. A.; Hohenester, E. *J. Biol. Chem.* **2008**, *283*, 16226−16234. (b) Li, Z.; Moniz, H.; Wang, S.; Ramiah, A.; Zhang, F.; Moremen, K. W.; Linhardt, R. J.; Sharp, J. S. *J. Biol. Chem.* **2015**, *290*, 10729−10740.
(15) Powell, A. K.; Ahmed, Y. A.; Yates, E. A.; Turnbull, J. E. *Nat. Protoc.* **2010**, *5*, 821−833.
(16) Ferreras, C.; Rushton, G.; Cole, C. L.; Babur, M.; Telfer, B. A.; van Kuppevelt, T. H.; Gardiner, J. M.; Williams, K. J.; Jayson, G. C.; Avizienyte, E. *J. Biol. Chem.* **2012**, *287*, 36132−36146.
(17) Zhang, F.; Moniz, H. A.; Walcott, B.; Moremen, K. W.; Wang, L.; Linhardt, R. J. *Glycoconjugate J.* **2014**, *31*, 299−307.
(18) Naimy, H.; Leymarie, N.; Bowman, M. J.; Zaia, J. *Biochemistry* **2008**, *47*, 3155−3161.
(19) Maxwell, E.; Tan, Y.; Tan, Y.; Hu, H.; Benson, G.; Aizikov, K.; Conley, S.; Staples, G. O.; Slysz, G. W.; Smith, R. D.; Zaia, J. *PLoS One* **2012**, *7*, e45474.
(20) (a) Huang, R.; Liu, J.; Sharp, J. S. *Anal. Chem.* **2013**, *85*, 5787−5795. (b) Huang, R.; Zong, C.; Venot, A.; Chiu, Y.; Zhou, D.; Boons, G. J.; Sharp, J. S. *Anal. Chem.* **2016**, *88*, 5299−5307.
(21) Chiu, Y.; Huang, R.; Orlando, R.; Sharp, J. S. *Mol. Cell. Proteomics* **2015**, *14*, 1720−1730.
(22) (a) Poletti, L.; Lay, L. *Eur. J. Org. Chem.* **2003**, *2003*, 2999−3024. (b) Noti, C.; de Paz, J. L.; Polito, L.; Seeberger, P. H. *Chem. - Eur. J.* **2006**, *12*, 8664−8686. (c) Arungundram, S.; Al-Mafraji, K.; Asong, J.; Leach, F. E., III; Amster, I. J.; Venot, A.; Turnbull, J. E.; Boons, G. J. *J. Am. Chem. Soc.* **2009**, *131*, 17394−17405. (d) Baleux, F.; Loureiro-Morais, L.; Hersant, Y.; Clayette, P.; Arenzana-Seisdedos, F.; Bonnaffe, D.; Lortat-Jacob, H. *Nat. Chem. Biol.* **2009**, *5*, 743−748. (e) Hu, Y. P.; Lin, S. Y.; Huang, C. Y.; Zulueta, M. M. L.; Liu, J. Y.; Chang, W.; Hung, S. C. *Nat. Chem.* **2011**, *3*, 557−563. (f) Dulaney, S. B.; Huang, X. F. *Adv. Carbohydr. Chem. Biochem.* **2012**, *67*, 95−136. (g) Tanaka, H.; Tateno, Y.; Takahashi, T. *Org. Biomol. Chem.* **2012**, *10*, 9570−82. (h) Hansen, S. U.; Miller, G. J.; Cole, C.; Rushton, G.; Avizienyte, E.; Jayson, G. C.; Gardiner, J. M. *Nat. Commun.* **2013**, *4*, 2016. (i) Schworer, R.; Zubkova, O. V.; Turnbull, J. E.; Tyler, P. C. *Chem. - Eur. J.* **2013**, *19*, 6817−6823. (j) Yoshida, K.; Yang, B.; Yang, W.; Zhang, Z.; Zhang, J.; Huang, X. *Angew. Chem., Int. Ed.* **2014**, *53*, 9051−9058. (k) Dulaney, S. B.; Xu, Y. M.; Wang, P.; Tiruchinapally, G.; Wang, Z.; Kathawa, J.; El-Dakdouki, M. H.; Yang, B.; Liu, J.; Huang, X. F. *J. Org. Chem.* **2015**, *80*, 12265−12279. (l) Hansen, S. U.; Miller, G. J.; Cliff, M. J.; Jayson, G. C.; Gardiner, J. M. *Chem. Sci.* **2015**, *6*, 6158−6164.
(23) (a) Haller, M.; Boons, G. J. *J. Chem. Soc.-Perkin Trans.* **2001**, *1*, 814−822. (b) Prabhu, A.; Venot, A.; Boons, G. J. *Org. Lett.* **2003**, *5*, 4975−4978. (c) Zong, C.; Venot, A.; Dhamale, O.; Boons, G. J. *Org. Lett.* **2013**, *15*, 342−345.
(24) Zhu, T.; Boons, G. J. *Tetrahedron: Asymmetry* **2000**, *11*, 199−205.
(25) van den Bos, L. J.; Codee, J. D. C.; Litjens, R. E. J. N.; Dinkelaar, J.; Overkleeft, H. S.; van der Marel, G. A. *Eur. J. Org. Chem.* **2007**, *2007*, 3963−3976.
(26) Vibert, A.; Lopin-Bon, C.; Jacquinet, J.-C. *Tetrahedron Lett.* **2010**, *51*, 1867−1869.
(27) (a) Fujiwara, M.; Ghazizadeh, M.; Kawanami, O. *Vasc. Med.* **2006**, *11*, 115−121. (b) Zhang, B.; Dietrich, U. M.; Geng, J. G.; Bicknell, R.; Esko, J. D.; Wang, L. *Blood* **2009**, *114*, 4300−4309. (c) Chen, C. Y.; Tsai, C. H.; Chen, C. Y.; Wu, Y. H.; Chen, C. P. *Cell Adh. Migr.* **2016**, *10*, 66−76.

DOI: 10.1021/jacs.6b08161
J. Am. Chem. Soc. 2016, 138, 13059−13067